# Collective fast ion instability-induced losses in National Spherical Tokamak Experiment[a)]

E. D. Fredrickson,[b)] R. E. Bell, D. S. Darrow, G. Y. Fu, N. N. Gorelenkov, B. P. LeBlanc, S. S. Medley, J. E. Menard, H. Park, and A. L. Roquemore
*Princeton Plasma Physics Laboratory, Princeton, New Jersey 08543*

W. W. Heidbrink
*University of California, Irvine, California 92697*

S. A. Sabbagh
*Columbia University, New York, New York 10027-6902*

D. Stutman and K. Tritz
*Johns Hopkins University, Baltimore, Maryland 21218*

N. A. Crocker, S. Kubota, and W. Peebles
*University of California, Los Angeles, California 90095-1354*

K. C. Lee
*University of California, Davis, California 95616*

F. M. Levinton
*Nova Photonics, Princeton, New Jersey 08543*

(Received 31 October 2005; accepted 11 January 2006; published online 11 May 2006)

A wide variety of fast ion driven instabilities are excited during neutral beam injection (NBI) in the National Spherical Torus Experiment (NSTX) [Nucl. Fusion **40**, 557 (2000)] due to the large ratio of fast ion velocity to Alfvén velocity, $V_{\mathrm{fast}}/V_{\mathrm{Alfvén}}$, and high fast ion beta. The ratio $V_{\mathrm{fast}}/V_{\mathrm{Alfvén}}$ in ITER [Nucl. Fusion **39**, 2137 (1999)] and NSTX is comparable. The modes can be divided into three categories: chirping energetic particle modes (EPM) in the frequency range 0 to 120 kHz, the toroidal Alfvén eigenmodes (TAE) with a frequency range of 50 kHz to 200 kHz, and the compressional and global Alfvén eigenmodes (CAE and GAE, respectively) between 300 kHz and the ion cyclotron frequency. Fast ion driven modes are of particular interest because of their potential to cause substantial fast ion losses. In all regimes of NBI heated operation we see transient neutron rate drops, correlated with bursts of TAE or fishbone-like EPMs. The fast ion loss events are predominantly correlated with the EPMs, although losses are also seen with bursts of multiple, large amplitude TAE. The latter is of particular significance for ITER; the transport of fast ions from the expected resonance overlap in phase space of a "sea" of large amplitude TAE is the kind of physics expected in ITER. The internal structure and amplitude of the TAE and EPMs has been measured with quadrature reflectometry and soft x-ray cameras. The TAE bursts have internal amplitudes of $\tilde{n}/n=1\%$ and toroidal mode numbers $2<n<7$. The EPMs are core localized, kink-like modes similar to the fishbones in conventional aspect ratio tokamaks. Unlike the fishbones, the EPMs can be present with $q(0)>1$ and can have a toroidal mode number $n>1$. The range of the frequency chirp can be quite large and the resonance can be through a fishbone-like precessional drift resonance, or through a bounce resonance. © *2006 American Institute of Physics*.
[DOI: 10.1063/1.2178788]

## I. INTRODUCTION

Thermonuclear plasmas are heated by the products of the D-T fusion reaction, 3.5 MeV $He^{++}$, or $\alpha$'s, which are much more energetic than the particles in the thermal plasma. The addition of a large population of energetic, nonthermal, particles to the thermal plasma provides a source of energy, which may excite waves and instabilities. The energy available to excite the waves and instabilities from these nonthermal populations is in the gradients of particle density in real or phase (velocity) space. The resonances that can couple this energy to waves are many, and are identified by the characteristic frequencies or combinations of frequencies involved; including the diamagnetic drift frequency, the precession and bounce frequencies of trapped particles, the passing frequency, and the cyclotron frequency. This broad range of possible resonances allows coupling to a wide range of waves.

The heating of plasmas in contemporary tokamaks with neutral beams and many forms of radio frequency wave heating also introduce large nonthermal fast ion populations. These fast ion populations can simulate some predicted be-

[a)]Paper QI1 5, Bull. Am. Phys. Soc. **50**, 259 (2005).
[b)]Invited speaker.

 

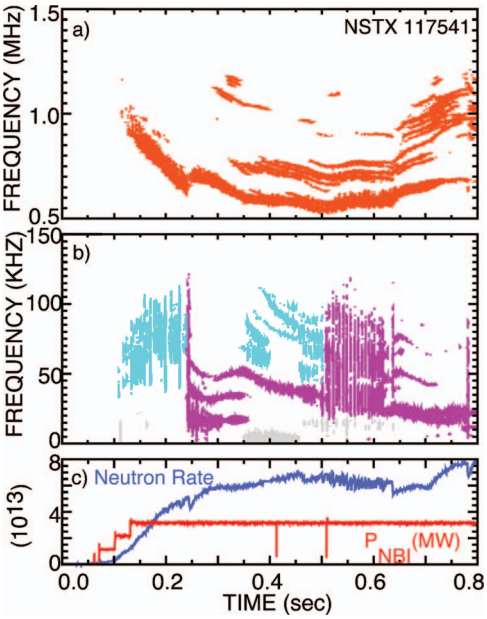


FIG. 1. (Color) Magnetic fluctuations in a typical NSTX beam heated plasma. (a) Compressional and global Alfvén eigenmodes (orange); (b) toroidal Alfvén eigenmodes (cyan) and energetic particle modes (magenta); (c) neutral beam heating power (red) and a global neutron rate (blue).

haviors of the fusion $\alpha$'s in thermonuclear plasmas. Many of the waves expected to be excited by the fast ion population are Alfvénic, that is, waves where the magnetic field provides the restoring force to the inertia of the plasma. The neutral beam ions in National Spherical Torus Experiment (NSTX)[1] have a velocity several times higher than the characteristic velocity of Alfvén waves, $V_A$, similar to the ratio of the fusion $\alpha$ velocity to $V_A$ in the International Thermonuclear Experimental Reactor, ITER.[2] Similarly, the relative density of beam ions in NSTX, $\beta_{NBI}/\beta_{thermal}$, is comparable to or larger than $\beta_\alpha/\beta_{thermal}$ in ITER. However, no currently operating device can simultaneously match all of the relevant ITER dimensionless parameters, chief among those is the fast ion Larmor radius normalized to the plasma minor radius, $\rho^* = \rho/a$.

The NSTX is a low aspect ratio ($R_{major}/r_{minor} \approx 0.85$ m/0.65 m) toroidal device. The range of operational parameters used for the experiments discussed here are 0.7 to 1.2 MA of toroidal plasma current, 3.0 to 4.5 kG toroidal field, central electron density of $1.5-8\times 10^{19}/m^3$, central electron temperature of up to $\approx 1$ keV. The plasmas were heated with 1.5 to 6 MW of deuterium neutral beam injection (NBI) power at a full energy as high as 90 kV.

A much richer spectrum of fast ion instabilities are excited in the NSTX than has been the case for conventional aspect ratio devices. Fast ion driven instabilities excited during neutral beam injection heating in NSTX have frequencies ranging from the ion cyclotron frequency down to magnetohydrodynamic (MHD) frequencies (Fig. 1). In the lowest frequency range [0 to 120 kHz in Fig. 1(b)] are energetic particle modes, EPM[3–6] shown in magenta. These are modes with relatively strong drive and damping; which means that the mode frequency is governed primarily by the interaction of the mode with the fast ion population, i.e., the mode has the frequency that optimizes energy transfer from the fast ions to the mode. These modes often exhibit strong frequency chirping, i.e., as the fast ion population is depleted by the mode, the mode frequency drops to maintain optimum energy transfer.

At higher frequency [50 to 200 kHz in Fig. 1(b)] are the toroidal Alfvén eigenmodes, TAE.[7–10] shown in cyan. These modes are weakly damped natural resonant frequencies of the plasma, much like the natural oscillation frequency of a violin string. These modes need only be weakly driven, however, the nature of the resonant interaction still allows, under some conditions, for substantial losses of fast ions. The TAE may, of course, be strongly driven, in which case the frequency can be shifted from the natural resonant frequency. We classify, here, modes in the TAE frequency range that exhibit chirping as resonant toroidal Alfvén eigenmodes, rTAE.[11–15]

Finally, in the 300 kHz to >3 MHz frequency range, two additional types of modes are seen [Fig. 1(a)], the compressional and the global Alfvén eigenmodes (CAE and GAE, respectively, both in orange).[16–25] These are also weakly damped natural modes of the plasma and exhibit behavior similar to that of the TAE. The GAE are shear waves ($\delta B$ perpendicular to the equilibrium field), but can couple to compressional waves. The CAE, as the name implies, are compressional waves, with $\delta B$ parallel to the equilibrium field, and thus with $\delta E$ perpendicular to the field. Because the electric field from the wave is transverse to $B_0$, the waves are limited to extracting perpendicular energy from the fast ions. In NSTX, the resonant drive for both the CAE and GAE is predominantly through the Doppler shifted cyclotron resonances. Thus, the CAE and GAE propagate counter to the beam injection direction, so that in the beam ion rest frame, the wave fields oscillate at the cyclotron frequency. Each of these categories of modes exhibits a wide range of behavior, including quasicontinuous behavior, bursting, chirping, and, except for the lower frequency range (EPM), turbulence.

Fast ion driven modes are of particular interest in fusion research because of their potential to cause transport, or even substantial losses, of the fast ions that heat the plasma. Fast ion losses will directly reduce the heating efficiency, but may also cause damage to plasma facing components through localized energy deposition. In NSTX beam heated plasmas we see transient neutron rate drops, correlated with bursts of fast ion driven instabilities, including modes identified as TAE and fishbone-like EPM.[26] The CAE and GAE may also affect fast ion confinement, but so far there is little direct evidence for the enhanced transport of fast ions in the presence of these instabilities.

Fast ion loss events, together with TAE and EPM, are seen in nearly all regimes of NSTX NBI heated operation, up to the highest $\beta$, highest densities, and at the highest plasma current. This contrasts the experience on the Mega-Ampere Spherical Tokamak (MAST), where TAE amplitudes were reduced in amplitude at high $\beta$.[27] In Fig. 2 is shown an existence plot for TAE or EPM activity in NSTX showing that $\beta_{fast}(0)/\beta_{tot}(0)$ decreases at high density and that EPM and TAE tend to be absent, where $\beta_f(0)/\beta_{tot}(0) < 0.3$ (Fig. 2,

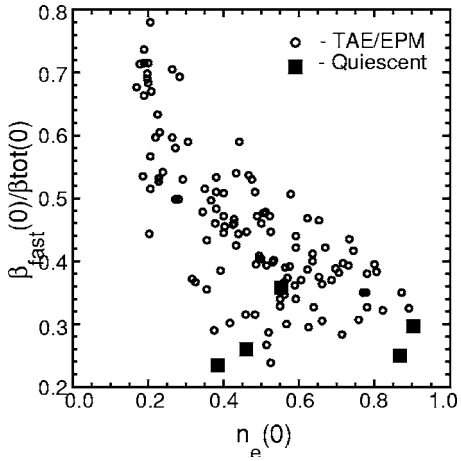


FIG. 2. (Color online) Existence plot for TAE/EPM activity. EPM/TAE present (blue) for $\beta_{\text{fast}}(0)/\beta_{\text{tot}}(0) > 30\%$, EPM/TAE absent (green) for $\beta_{\text{fast}}(0)/\beta_{\text{tot}}(0) < 30\%$.

green points). Fast-ion driven MHD activity can be reduced by operation at very high densities with low beam power, or with reduced beam voltage (<60 kV; typical injection energy is 80 to 90 kV), suggesting that the absence of TAE at high $\beta$ on MAST is due to their lower voltage beams.

## II. ENERGETIC PARTICLE MODES

Energetic particle modes are bursting modes where the frequency chirps down strongly during each burst. The mode frequency can change rapidly because the frequency is determined by the fast-ion distribution function, which the mode can change on the mode growth time scale. On NSTX, the EPM can have toroidal mode numbers from $n=1$ up to at least $n=5$. In Fig. 3, a series of five $n=1$ EPM bursts occurs between 0.3 s and 0.34 s, as well as an earlier burst at 0.245 s. The $n=1$ EPM are very similar to the "fishbone"

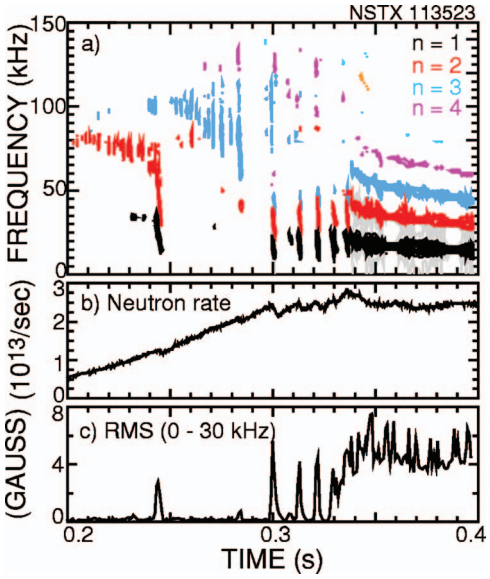


FIG. 3. (Color) Mirnov spectrogram showing $n=1$ EPMs (fishbones) between 0.3 and 0.34 s. In panel (b) the neutron trace indicates the loss of fast ions at each burst.

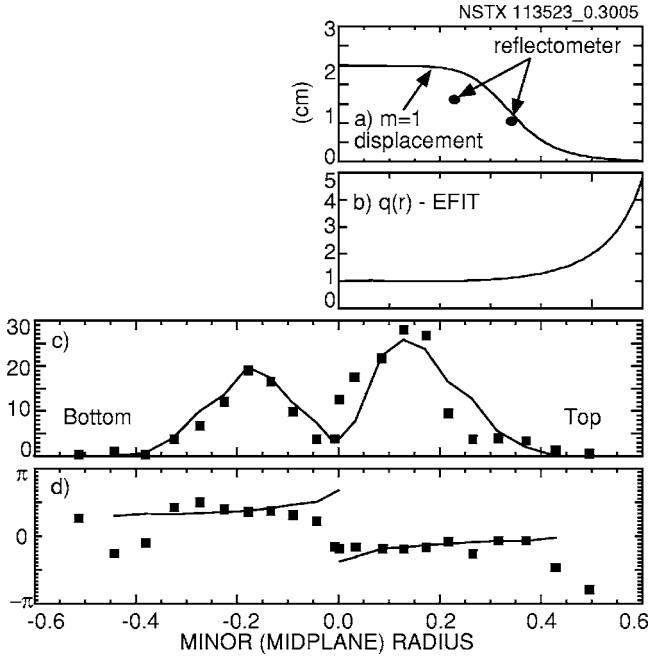


FIG. 4. The simulation of soft x-ray emissivity fluctuations for low frequency EPM. (a) trial eigenfunctions (solid line), local displacement measured with reflectometer (points); (b) MSE/EFIT $q$—profile, (c) simulated (solid line) and measured soft x-ray chord integrated emissivity fluctuations (black dots); (d) phase of fluctuations (solid line–simulation, black dots–experiment).

EPM first seen on the Poloidal Divertor Tokamak (PDX).[8] They most often occur when $q(0) \approx 1$, however, examples are seen where $q(0)$ is believed to be well above unity (e.g., Fig. 3, 0.245 s). In cases with an elevated $q(0)$ and a large low shear region, EPM with toroidal mode numbers greater than unity can be found.

The fishbone-like EPM have a core localized, kink-like structure, similar to conventional fishbones. The internal fluctuations are measured with soft x-ray cameras (chord integral data) and microwave reflectometers (local displacement). The chord integrated soft x-ray emission can, in principle, be inverted with tomographic techniques. However, due to the limited number of chords, a simpler approach is to model the soft x-ray data with a multiparameter eigenfunction. The technique used is to assume the local soft x-ray emissivity is a flux surface quantity and perform a simple Abel-type inversion using the equilibrium flux surface geometry calculated by EFIT [28,29] A trial eigenfunction for the mode is introduced in a perturbative sense, and the soft x-ray chords are reintegrated and compared to the time behavior of the original data. In Fig. 4, the soft x-ray chordal data are compared to data simulated with the assumption of an $m=1$, $n=1$ kink-like eigenfunction peaked on axis with a peak displacement of about 2.5 cm. In this example the multichannel heterodyne reflectometer was also used to measure the local mode displacement. For the mode shown in Fig. 4, the two reflectometer channels were fortuitously located near the minor radius of the inferred $q=1$ surface. The measured displacement agrees well with that inferred from the soft x-ray camera data. The soft x-ray data were from two cameras

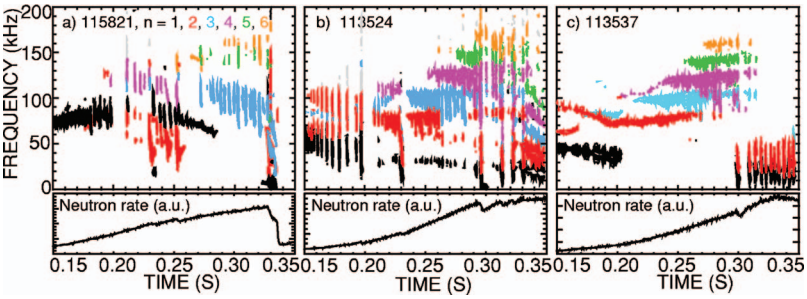


FIG. 5. (Color) Spectrogram of magnetic fluctuations for three shots showing "low" frequency fast ion driven instabilities, including toroidal Alfvén eigenmodes and various forms of energetic particle (chirping) modes.

located on the outboard midplane, looking at the upper and lower halves of the plasma, respectively.

The $n>1$ EPM chirps start in the first shear-Alfvén gap, near the TAE frequency. These EPMs may be related to a TAE-like mode that can exhibit frequency chirping, the rTAE, or to the Infernal Fishbone.[30] The connection to the TAE can be seen in Figs. 5(a)–5(c), where spectrograms of magnetic fluctuations are shown for three beam heated discharges. The energetic particle modes in the first shot [Fig. 5(a)] are discrete bursts with strong frequency chirping ($\delta f \approx 50$ kHz). The bursts in the second example [Fig. 5(b)] are starting to overlap, and the frequency chirp weakens, but clearly starts at the TAE frequency. In the final example [Fig. 5(c)], the EPM appear as only intermittent chirps during quasicontinuous TAE activity. The large Doppler shift makes mode identification based on frequency ambiguous. These higher-$n$ EPMs, as well as TAE, tend to be suppressed during low frequency EPM activity [Fig. 1(b)]. The presence of high frequency EPMs appears to be correlated with elevated $q(0)$, or shear reversal, although the number of shots with MSE measurement of the $q$ profile is limited at this time.

The fast chirping suggests a nonlinear resonant interaction similar to that for the conventional aspect ratio tokamak fishbone. However, the precession-drift frequency, the resonant interaction responsible for the fishbone chirp, is often too low on NSTX to explain the high frequency of these EPMs. The resonance believed responsible for the high frequency EPMs is with the fast ion bounce frequency.[31] The bounce-resonance drive can be stronger at low aspect ratio in part because the average bounce angle is high.

The internal structure of the high-$n$ EPM can be reconstructed from soft x-ray data as for the $n=1$ EPM. In Fig. 6 is shown a simulation of the soft x-ray data for an $n=2$ EPM seen in Fig. 5(a) at 0.253 s. The $q$ profile at this time, from EFIT and MSE data, shows weak shear reversal, with $q_{min} \approx 1.5$. The simulations indicate that the peak mode displacement amplitude is $\approx 3.5$ cm and probably localized near the $q_{min}$ surface. The data were fit with a combination of $m=5$, $m=4$, and $m=3$ modes, however there is substantial uncertainty in this type of reconstruction. The x-ray profile is somewhat hollow and sensitivity to mode structure is low in the core.

In Fig. 6 the MSE measurement of the $q$ profile indicates $q>1.5$ and weakly reversed, in other shots it is believed that the $q$ profile is more strongly reversed, similar to what is found in the presence of cascade modes. However, the rate of the frequency chirp, the direction, and the general characteristics of the frequency chirping EPM are substantially different from what has been reported for cascade modes elsewhere.[32] The absence of the cascade modes is curious; it is possible that the energetic particle mode is more strongly unstable, and thus responsible for the suppression of the cascade modes in NSTX.

## III. TOROIDAL ALFVÉN EIGENMODES

Toroidal Alfvén eigenmodes are seen in most operational regimes on NSTX, including shots with $\beta_{tor}$ up to 35%. An example from a shot, which reached a peak toroidal $\beta$ of >35%, is shown in Fig. 7. As seen in this figure, the TAE typically manifest as a sequence of short bursts, which often exhibit weak downward frequency chirps. The spectrum of TAE often appears incoherent or turbulent, with modes growing and decaying on a submillisecond time scale. In this example the $n=3$ and $n=4$ TAE were predominant. Several bursts of lower frequency chirping modes are also seen, and the two indicated resulted in substantial fast ion losses seen as abrupt neutron rate drops. The third event at $\approx 0.23$ s did not result in a significant neutron rate drop, however, it was

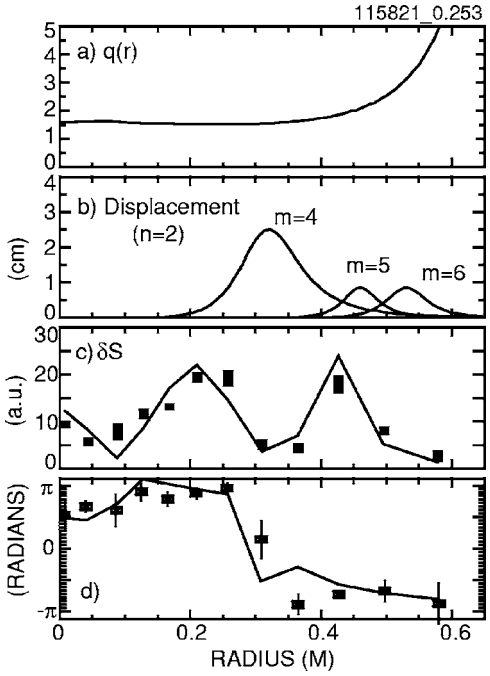


FIG. 6. Simulation of soft x-ray emissivity fluctuations for high frequency EPM. (a) MSE/EFIT $q$ profile; (b) trial eigenfunctions; (c) simulated and measured soft x-ray chord integrated emissivity fluctuations; (d) phase of fluctuations (simulations shown by solid lines, experimental data by symbols).

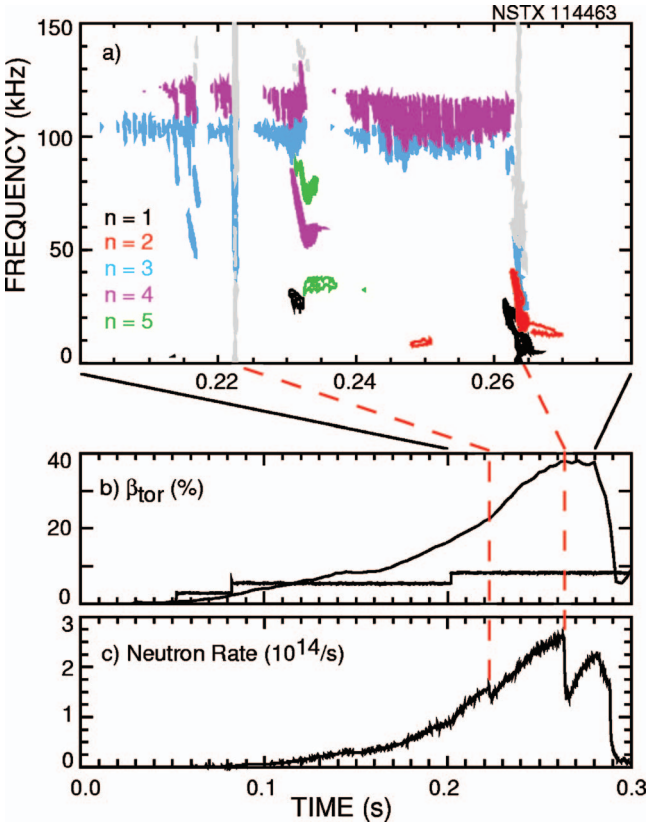


FIG. 7. (Color) (a) Spectrogram showing TAE (and EPM) activity in a high $\beta$ NSTX plasma; (b) toroidal beta and neutral beam heating power; (c) neutron rate.

followed by a period of weaker TAE activity, suggesting that even though fast ions might not have been expelled from the plasma, there was redistribution in either real or velocity space.

The observation of TAE activity in even the highest beta NSTX plasmas is in contrast to the experience on MAST. As $\beta_{\text{tor}}$ on MAST approaches 20%, the TAE activity becomes weaker. This difference in behavior most likely results from the much higher energy neutral beams used on NSTX, typically 90 kV or higher in the high performance plasmas. The ratio of fast ion beta to thermal beta in even the highest $\beta$ plasmas on NSTX is still $\approx$30%.

For the most part, TAE activity on NSTX does not produce significant fast ion losses (as measured with the neutron diagnostic). However, transient neutron drops, signifying fast ion loss events, are correlated with strong TAE bursts. In Fig. 8 is shown an example where several such strong TAE bursts are correlated with drops in the neutron rate. Each of the strong bursts is preceded by a sequence of short, chirping bursts with three or four discrete TAE modes. The bursts have toroidal mode numbers from 3 to 5 or 6. This sequence culminates in a strong burst in which many TAE modes can be distinguished. The onset of the strong burst is abrupt, almost as if some threshold had been crossed.

In Fig. 9 are shown magnetic and density fluctuation spectra, measured by a Mirnov coil and reflectometer, respectively. The toroidal mode numbers for nine of the frequency peaks are indicated in the figure. The local density

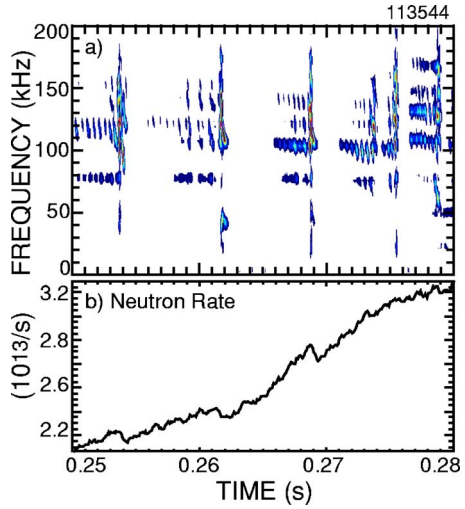


FIG. 8. An example of TAE-induced fast ion losses. (a) Mirnov spectrogram showing weak TAE chirping bursts leading to strong bursts; (b) neutron rate showing drops at major TAE bursts.

fluctuation amplitudes are measured with a multichannel reflectometer and the strongest modes have an amplitude, $\delta n/n \leqslant 1\%$. These bursts are suggestive of the "sea of TAE" modes expected in ITER.

The profile information for the $n=5$ mode at 136.7 kHz is shown in Fig. 10. In Fig. 10(a) the mode amplitude as measured with the three reflectometer channels is shown, showing the strongest fluctuations toward the plasma core. For this mode there is a phase inversion, Fig. 10(b), toward the plasma edge, consistent with Nova modeling of the higher $n$ TAE. The strong drive for TAE, from the high fast ion beta is hypothesized to drive TAE to sufficient amplitude, such that there is overlap in the phase space of the resonant interaction of fast ions with the TAE, i.e., the domino effect. The transport of fast ions in the presence of similar multiple TAE has been postulated as a fast ion loss mechanism for ITER, although present simulations suggest that fast ion transport due to TAE will be small.[33]

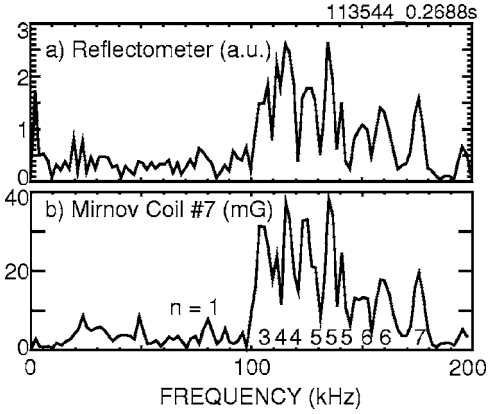


FIG. 9. Spectra of (a) local density fluctuations at $R=1.32$ m from the reflectometer and (b) magnetic fluctuations where toroidal mode numbers for selected peaks are indicated.

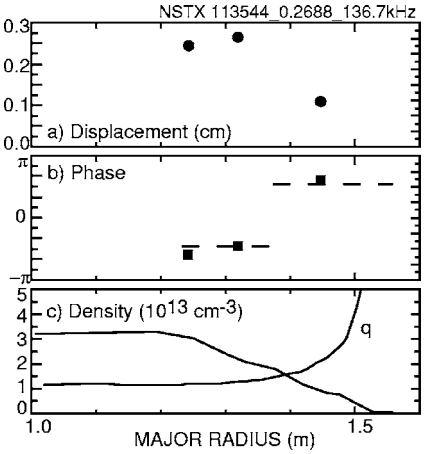


FIG. 10. The radial profile of 136.7 kHz, $n=5$ TAE fluctuation amplitude measured with a reflectometer. (a) The profile of fluctuation amplitude; (b) the profile of phase showing phase inversion toward the edge; and (c) the profile of density and $q$.

## IV. COMPRESSIONAL AND GLOBAL ALFVÉN MODES

A complex range of behavior is seen in the global and compressional Alfvén mode range of frequencies, $0.2\omega_{ci} < \omega < \omega_{ci}$. In addition to the discrete, hierarchical frequency spectrum discussed in some of the earlier papers on CAE,[34] modes in this frequency range are also seen to have bursting, chirping behavior, or sometimes a broad, turbulent spectrum and sometimes discrete modes, with a range of frequencies that are not particularly evenly spaced. Some of this variation in behavior may be explained by the relative strength of the fast ion drive, as described by Breizman *et al.*[35] In particular, the broad, turbulent spectrum of modes often seen is suggestive of a strongly driven regime where the normally discrete spectrum of modes broadens in response to the condition where $\gamma \approx \omega$.

An array of Mirnov coils was installed on NSTX to measure the toroidal mode numbers and polarization of the high frequency modes. The polarization here refers to the perpendicular versus parallel alignment of the perturbed field relative to the equilibrium field. The polarization will, in general, be elliptical, which includes as limiting cases linear polarization, either parallel or perpendicular, to the equilibrium field (or at some arbitrary angle). Three examples of the measured wave polarization are shown in Fig. 11 for a low frequency EPM, a wave believed to be a GAE and a wave believed to be a CAE. The low frequency modes (MHD kinks, tearing modes, EPM and TAE) have shear polarization, as expected. The GAE exhibits elliptical polarization, meaning the wave electric field has components aligned both parallel and perpendicular to the equilibrium field. Finally, the CAE has nearly a linear polarization aligned close to the equilibrium field (within experimental uncertainty).

Many of the basic characteristics of the CAE and GAE have been explored in previous papers. Here, we will focus on the interesting observations of bursting and chirping often seen early in the NBI heating phase. In Fig. 12(a) is shown a spectrogram of Mirnov coil data showing a sequence of high frequency bursts during the early period of an NSTX plasma.

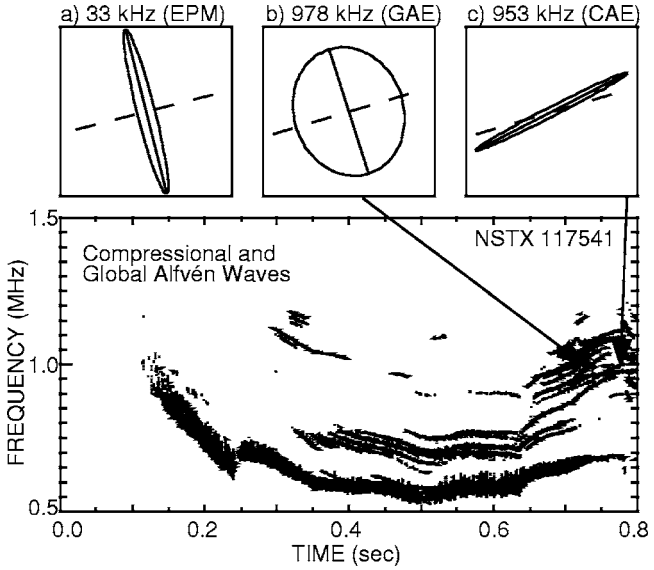


FIG. 11. Polarization for the selection of fast ion driven modes. (a) A33 kHz energetic particle mode showing shear polarization; (b) 978 kHz global Alfvén eigenmode showing mixed shear and compressional polarization; and (c) 953 kHz compressional Alfvén eigenmode showing compressional polarization. The dashed line shows the pitch of the equilibrium field on the outboard midplane at the 90% flux surface.

Neutral beam injection heating starts at 0.06 s and the plasma current does not reach a 1.2 MA flattop phase until about 0.3 s. The bursting, chirping modes are seen between 300 and 700 kHz.

A single burst is further expanded in Fig. 12(b). In this example the mode chirps both up and down in frequency over a frequency range of about 150 kHz, or $\delta f/f_0 \approx 30\%$.

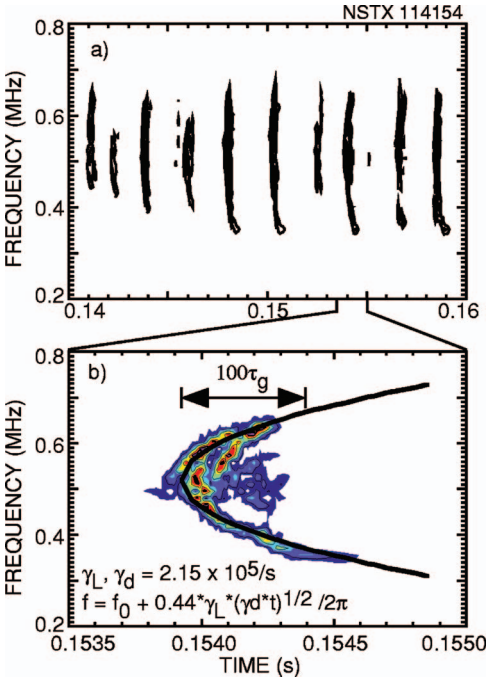


FIG. 12. (Color) Spectrogram detail of bursting GAE modes (Angelfish) during early NBI heating during current ramp-up. (a) A spectrogram showing the sequence of GAE bursts; (b) expanded view of a single burst showing simultaneous up down chirp.

"Inside" the main mode peaks are a set of secondary modes, possibly excited by the changes in the fast ion distribution resulting from this event. The downward chirping component lasts longer, but has a smaller amplitude than the upward chirping component. Similar events have also been seen where only the downward (or more rarely, upward) chirp is seen.

The chirp event in Fig. 12(b) lasts about 0.7 ms. In a discharge with twice the beam heating power, the chirp events are shorter, lasting perhaps 0.3 ms. The modes in both cases propagate in the counter, $\omega_{*e}$, direction and the toroidal mode numbers for both the upward and downward chirps are measured to be $n=5$. The polarization of the mode (shear versus compressional) as measured at the vacuum vessel wall suggests that the mode has mixed polarization, consistent with expectations for the global Alfvén eigenmode (GAE). No information on the poloidal structure is presently available.

The chirping of the GAE is not normally expected, as the GAE is a weakly damped resonant mode of the plasma and the frequency of the mode should be, to first order, determined by the thermal plasma parameters. However, in the theory proposed by Berk, Breizman, and Petviashvili[36–38] for the spontaneous generation of hole-clump pairs, albeit for a one-dimensional (1-D) bump-on-tail resonant interaction, would predict exactly this type of behavior. In this theory, the nonlinear interaction of a marginally unstable resonant mode with a collisionless, inverted fast-particle distribution results in the splitting of the mode frequency, and upward and downward frequency chirping as the "holes" and "clumps" formed in the distribution function propagate in particle phase space. The theory predicts (for $\delta\omega/\omega_0 \ll 1$) that the frequency chirps follow the simple expression $\omega = \omega_0 \pm 0.44\gamma_L(\gamma_D t)^{1/2}$. The theory further predicts the formation of hole-clump pairs only for modes close to the marginal point, so for simplicity in Fig. 12 it was assumed that $\gamma_L \approx \gamma_D$, reducing the expression to a single parameter fit.

As the modes chirp, they retain their physical shape, i.e., $k_\parallel$ is constant. Thus, as the frequency sweeps, the mode-particle resonance will also sweep through the fast ion distribution. In the theory of hole clumps, the fast ion diffusion in velocity space, e.g., from collisions, will tend to erase the holes and clumps, eventually limiting the extent of the frequency sweep in a time $\tau = \gamma_L^2/\nu_{\text{eff}}^3$. In Fig. 13, showing the fast ion distribution function, the red curve indicates fast ions that satisfy the resonance constraint at the initial mode frequency. The two blue curves indicate the resonance constraint at the extremes of the frequency sweep, seen in the inset. So in this example, as the chirps last about 100 linear growth times, it appears that the frequency chirps are limited by the size of the bump-on-tail and we may only conclude that $\nu_{\text{eff}} \leqslant 0.2\gamma_L$.

It has been proposed and demonstrated that wave heating of the fast ion distribution can enhance the effective collisionality, suppressing the hole-clump behavior.[39] A similar experiment on NSTX was carried out where high harmonic fast wave heating (HHFW) was used to heat the beam ions. When such heating was applied during a period of hole-clump activity, the amplitude and duration of the bursts was significantly reduced (Fig. 14). Thus, while the hole-clump theory of Berk, Breizman, and Petviashvili may not be directly applicable to these modes, some of the predictions of the theory seem to be surprisingly robust.

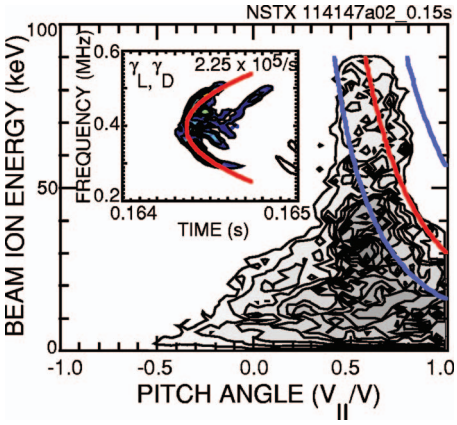


FIG. 13. (Color) Fast ion distribution function as calculated by TRANSP with a Doppler-shifted ion-cyclotron resonance constraint indicated by a red line for the initial frequency of GAE burst. The two blue lines show the resonance constraint corresponding to the minimum and maximum of the chirp frequencies. (The inset shows the actual GAE burst.)

## V. SCALING OF LOSSES

Fast ion loss events are most often correlated with chirping modes, either the low frequency fishbone-like modes, intermediate frequency EPMs, or bursts of multiple, weakly chirping, $\delta f/f \leqslant 20\%$, TAE modes; possibly resonant TAE (rTAE). The neutron production is predominantly from beam-target interactions, so the fractional neutron rate drop is approximately the fast ion loss fraction. The fractional neutron rate drop scales loosely with the normalized amplitude of the energetic particle modes in Fig. 15 (blue). A similar scaling has been found for TAE induced losses, the red points in Fig. 15. In this case many loss events were sorted to find those where EPM activity was very weak or undetectable. The scaling is similar, but a similar loss frac-

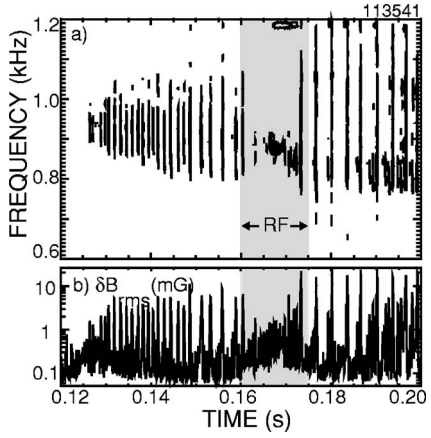


FIG. 14. Suppression of the Angelfish by the application of rf heating (grey band), in panel (a) is a spectrogram showing the GAE bursts and in (b) is the rms magnetic fluctuation level showing a reduction in amplitude during rf heating.

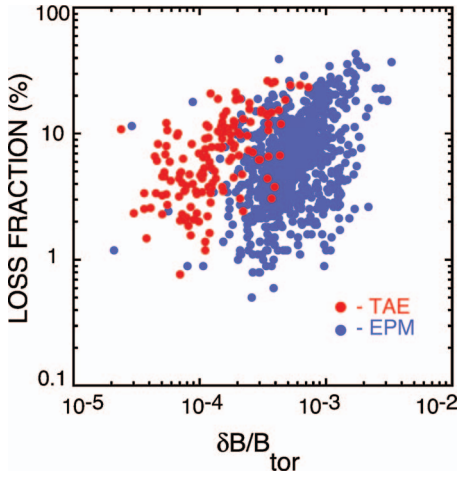


FIG. 15. (Color) The scaling of the fast ion loss fraction (percent drop in neutron rate) with amplitude of TAE (red) and EPM (blue).

tion is seen for comparatively weaker modes in the TAE case. This might suggest that either the TAE are more core localized, or that they more efficiently transport fast ions.

## VI. CONCLUSIONS

A broad spectrum of fast ion driven instabilities are excited in NSTX by the super-Alfvénic neutral beam ions. These modes include energetic particle modes, toroidal Alfvén eigenmodes, resonant toroidal Alfvén eigenmodes, and high frequency compressional and global Alfvén eigenmodes. The polarization of the compressional and global Alfvén waves has been measured. Of these instabilities, the frequency chirping EPMs are most likely to cause fast ion losses, followed by TAE. No clear evidence for fast ion losses correlated with CAE or GAE activity has been found.

The fast ion loss fraction for both EPM and TAE bursts is found to scale approximately linearly with mode amplitude. No clear scaling of loss fraction with plasma current or plasma beta is seen. The TAE bursts responsible for significant fast ion losses contain many independent modes with amplitudes as large as $\delta n/n \approx 1\%$. This is similar to the "sea of Alfvén mode" condition predicted for ITER. TAE are seen in even the highest beta NSTX plasmas, in contrast to observations on MAST. However, for plasmas where $\beta_{\mathrm{fast}}/\beta_{\mathrm{tot}}(0) < 20\%$ the fast ion driven instabilities are much weaker or absent. The difference is attributed to the higher energy neutral beams on NSTX.

The GAE and CAE seen on NSTX are predicted to be excited through a Doppler-shifted ion-cyclotron resonance with the fast beam ions. This requires a bump on tail in the perpendicular direction. The preceding analysis has found that the TRANSP calculation of the fast ion distribution predicts the presence of a perpendicular bump on tail and that this tail includes fast ions resonant with the observed GAE modes. The measured wave propagation direction is consistent with the Doppler shifted resonance condition, the waves need to propagate in the counter, $\omega^*_e$, direction. And, using a simple dispersion relation for the GAE, it is possible to match both the mode frequency and show that fast ions in the bump on tail are resonant with the GAE mode.

The frequency evolution of the chirping modes is consistent with the hole-clump pair model proposed by Berk, Breizman, and Petviashvili, but is in the unique paradigm of the Doppler-shifted ion-cyclotron resonance driven global Alfvén eigenmode. The linear growth rate inferred from the hole-clump model based on the frequency chirps is fairly large. The time duration of the frequency chirps is comparable to that found for the numerical simulations, $\approx 100/\gamma_L$, but in this case the duration seems to be set not so much by the effective collision rate in the fast ion distribution, but by the extent of the bump on tail. Generally the results of the analysis suggest that the observed behavior is consistent with a Doppler-shifted ion-cyclotron resonance driven GAE mode, resulting in the formation of hole-clump pairs. However, the possibility that these bursts are CAE is not excluded.

## ACKNOWLEDGMENT

This work is supported by U.S. DOE Contract No. DE-AC02-76CH03 073.

[1] M. Ono, S. M. Kaye, Y-K. M. Peng *et al.*, Nucl. Fusion **40**, 557 (2000).
[2] ITER Physics Basis Editors, ITER Expert Group Chairs and Co-Chairs, ITER Joint Central and Physics Integration Unit, ITER EDA, Naka Joint Work Site, Mukouyama, Naka-machi, Maka-gun, Ibaraki-ken, Japan, Nuclear Fusion, 1999, Vol. 39, p. 2137.
[3] K. M. McGuire, R. Goldston, M. Bell *et al.*, Phys. Rev. Lett. **50**, 891 (1983).
[4] PDX Group, Princeton Plasma Physics Laboratory, Phys. Rev. Lett, 1983, Vol. 50, p. 891.
[5] R. B. White, R. J. Goldston, K. M. McGuire *et al.*, Phys. Fluids **26**, 2958 (1983).
[6] L. Chen, R. B. White, and M. N. Rosenbluth, Phys. Rev. Lett. **52**, 1122 (1984).
[7] C. Kieras and J. Tataronis, J. Plasma Phys. **28**, 395 (1982).
[8] C. Z. Cheng and M. S. Chance, Phys. Fluids **29**, 2471 (1986).
[9] K. L. Wong, R. J. Fonk, S. F. Paul *et al.*, Phys. Rev. Lett. **66**, 1874 (1991).
[10] W. W. Heidbrink, E. J. Strait, E. Doyle, G. Sager, and R. T. Snider, Nucl. Fusion **31**, 1635 (1991).
[11] L. Chen, Phys. Plasmas **1**, 1519 (1994).
[12] C. Z. Cheng, N. N. Gorelenkov, and C. T. Hsu, Nucl. Fusion **35**, 1639 (1995).
[13] F. Zonca and L. Chen, Phys. Plasmas **3**, 323 (1996).
[14] E. D. Fredrickson, M. G. Bell, R. Budny, Z. Chang, C. Z. Cheng, G. Y. Fu, E. Mazzucato, R. Nazikian, A. T. Janos, K. M. McGuire, R. Majeski, C. K. Phillips, G. Schilling, G. Taylor, and J. R. Wilson, Nucl. Fusion **35**, 1457 (1995).
[15] S. Bernabei, M. G. Bell, R. V. Budny, E. D. Fredrickson, N. N. Gorelenkov, J. C. Hosea, R. Majeski, E. Mazzucato, C. K. Phillips, G. Schilling, and J. R. Wilson, Phys. Rev. Lett. **84**, 1212 (2000).
[16] K. Appert, R. Gruber, F. Troyon, and J. Vaclavik, Plasma Phys. **24**, 1147 (1982).
[17] D. W. Ross, G-L. Chen, and S. M. Mahajan, Phys. Fluids **25**, 652 (1982).
[18] S. M. Mahajan, D. W. Ross, and G-L. Chen, Phys. Fluids **26**, 2195 (1983).
[19] S. M. Mahajan and D. W. Ross, Phys. Fluids **26**, 2561 (1983).
[20] B. Coppi, S. Cowley, R. Kulsrud, P. Detragiache, and F. Pegoraro, Phys. Fluids **29**, 4060 (1986).
[21] J. W. Van Dam, G. Fu, and C. Z. Cheng, Fusion Technol. **18**, 461 (1990).
[22] N. N. Gorelenkov and C. Z. Cheng, Nucl. Fusion **35**, 1743 (1995).
[23] N. N. Gorelenkov and C. Z. Cheng, Phys. Plasmas **2**, 1961 (1995).
[24] E. D. Fredrickson, N. Gorelenkov, C. Z. Cheng, R. Bell, D. Darrow, D. Johnson, S. Kaye, B. LeBlanc, J. Menard, S. Kubota, and W. Peebles, Phys. Rev. Lett. **87**, 145 001 (2001).
[25] N. N. Gorelenkov, C. Z. Cheng, E. Fredrickson, E. Belova, D. Gates, S. Kaye, G. J. Kramer, R. Nazikian, and R. B. White, Nucl. Fusion **42**, 977 (2002).

[26]E. D. Fredrickson, C. Z. Cheng, D. Darrow *et al.*, Phys. Plasmas **10**, 2852 (2003).
[27]M. P. Gryaznevich and S. E. Sharapov, Plasma Phys. Controlled Fusion **46**, S15 (2004).
[28]L. L. Lao, H. St John, R. D. Stambaugh, A. G. Kellman, and W. P. Pfeiffer, Nucl. Fusion **25**, 1611 (1985).
[29]S. A. Sabbagh, S. M. Kaye, J. E. Menard *et al.*, Nucl. Fusion **41**, 1601 (2001).
[30]Ya. I. Kolesnichenko, V. S. Marchenko, and R. B. White, PPPL Report PPPL-3786, 2003, submitted to Phys. Plasmas.
[31]E. D. Fredrickson, L. Chen, and R. B. White, Nucl. Fusion **43**, 1258 (2003).
[32]S. E. Sharapov, B. Alper, J. Fessey *et al.*, Phys. Rev. Lett. **93**, 165001 (2004).
[33]J. Jacquinot, S. Putvinski, G. Bosia, A. Fukuyama, R. Hemsworth, S. Konovalov, Y. Nagashima, W. M. Nevins, K. Rasumova, F. Romanelli, K. Tobita, K. Ushigusa, J. W. Van Dam, V. Vdovin, S. Zweben, H. L. Berk, D. Borba, B. N. Breizman, R. Budny, J. Candy, C. Z. Cheng, C. Challis, A. Fasoli, G. Y. Fu, W. Heidbrink, R. Nazikian, G. Martin, F. Porcelli, M. Redi, M. N. Rosenbluth, G. Sadler, S. E. Sharapov, D. A. Spong, R. White, F. Zonca, F. W. Perkins, D. E. Post, N. A. Uckan, M. Azumi, D. J. Campbell, N. Ivanov, M. Wakatani, and M. Shimada, Nucl. Fusion **39**, 2471 (1999).
[34]E. D. Fredrickson, N. N. Gorelenkov, and J. Menard, Phys. Plasmas **11**, 3653 (2004).
[35]H. L. Berk, B. N. Breizman, and M. Pekker, Phys. Plasmas **2**, 3007 (1995).
[36]H. L. Berk, B. N. Breizman, J. Candy, M. Pekker, and N. V. Petviashvili, Phys. Plasmas **6**, 3102 (1999).
[37]H. L. Berk, B. N. Breizman, and N. V. Petviashvili, Phys. Lett. A **A 234**, 213 (1997).
[38]G. J. Kramer, M. Iwase, Y. Kusama, A. Morioka, M. Nemoto, T. Nishitani, K. Shinohara, S. Takeji, K. Tobita, T. Ozeki, C. Z. Cheng, G.-Y. Fu, and R. Nazikian, Nucl. Fusion **40**, 1383 (2000).
[39]D. Maslovsky, B. Levitt, and M. E. Mauel, Phys. Plasmas **10**, 1549 (2003).